Nano and dendritic structured carboranes and metallacarboranes: From materials to cancer therapy

Narayan S. Hosmane [a,*], Zhu Yinghuai [b,*], John A. Maguire [c], Wolfgang Kaim [d], Masao Takagaki [e]

[a] *Department of Chemistry and Biochemistry, Northern Illinois University, The Michael Faraday Labs, DeKalb, IL 60115, USA*
[b] *Institute of Chemical and Engineering Sciences, No. 1 Pesek Road, Jurong Island, Singapore 627833, Singapore*
[c] *Department of Chemistry, Southern Methodist University, Dallas, TX 75275, USA*
[d] *Institut für Anorganische Chemie, Universität Stuttgart, Pffenwaldring 55, Stuttgart D-70550, Germany*
[e] *Department of Neurosurgery, Aino College Hospital 4-5-4, Higashioda, Ibaraki City, Osaka 567-0012, Japan*

ARTICLE INFO

ABSTRACT

An account of the current research carried out in our laboratories is presented. Included is the incorporation of several group 14 elements into charge-compensated carboranes. These species present a bonding pattern not found in other main group carboranes. In addition to our continuing studies of the syntheses and structures of organometallic compounds, the use of these compounds as catalysts and catalyst precursors has been investigated. The isotopic exchange reactions between ^{10}B enriched boron hydrides with naturally abundant boranes catalyzed by Ru(0) nanoparticles has been studied. The Ru(0) nanoparticles were obtained by the reduction of $[CpRuCp^*RuCp^*]PF_6$ ($Cp^* = C_5Me_5$) with hydrogen and stabilized by the ionic liquid trihexyltetradecylphosphonium dodecylbenzenesulfonate [THTdP][DBS]. This was found to be an excellent, long lived catalyst for the exchange reaction of B-10 enriched diborane and naturally abundant decaborane(14). Other approaches to the production and use of nano-metal catalysts have also been explored. The reduction of the iridium carborane, $(PPh_3)_2IrH(7,8-C_2B_9H_{11})$ with hydrogen in the presence of trihexyltetradecylphosphonium methylsulfonate, [THTdP][MS], produced an Ir(0) nanoparticles that catalyzed the phenylborolation as did our Ir(sal = N-R = salicylaldiminato; COD = cyclooctadiene complex. Progress in the use of single wall carbon nanotubes (SWCNT) as boron delivery agents was also discussed.

© 2008 Elsevier B.V. All rights reserved.

1. Introduction

Our research has dealt with two important aspects of inorganic chemistry: our continued interest in the structure and properties of the heterocarboranes, and, more recently in the use of metallacarboranes as precursors in the syntheses of nano-metal catalysts. This Account summarizes some of our more important results.

One class of organometallic compounds that closely parallels the metallocenes are those in which the cyclopentadienide anion, $[C_5R_5]^-$, is replaced by a heteroborane. Boranes are mixed hydrides of boron and hydrogen where the boron atoms are contained in electron deficient clusters. These clusters usually are associated with high negative charges. For example the general formula for an n vertex closed structure (*closo*) is $[B_nH_n]^{2-}$, the more open borane structures have increasingly higher negative charges. As a result, these compounds are difficult to work with. However, if a three electron $[B-H]^-$ vertex is replaced by a neutral three electron

vertex, such as a [C–R] group, there is no change in structure, but the charge is decreased by one. Some of the most encountered heteroboranes are the dicarbaboranes (dicarborane) in which the cluster charge is decreased by two; the general formula for an $n + 2$ vertex *closo*-dicarborane is $C_2B_nH_{n+2}$. If the primary bonding atom of the group replacing a [H–B] vertex is a metal, the cluster is referred to as a metallaborane, or more likely to be encountered, a metallacarborane. There are a simple, elegant set of rules, culminating in the Polyhedral Skeletal Electron Pair counting rules, for predicting the structures of the heteroboranes from the composition of the clusters [1–5]. Most of the metallacarboranes in this account are those with the general formula, $MC_2B_nH_{n+2}$ ($n = 4, 9$) [5d], having pentagonal bipyramidal and icosahedral structures, respectively. These can be viewed as coordination complexes between the metal, M^{2+}, and a $[nido-C_2B_nH_{n+2}]^{2-}$ ligand, in which the metal group is bonded to the open C_2B_3 pentagonal face of the carborane, in much the same way as the cyclopentadienide, $[C_5R_5]^-$, bonds to metals in the metallocenes. Indeed, the primary metal-bonding carborane orbitals are a set of three, filled, π-type orbitals delocalized about the pentagonal face of the carborane that are very similar to those of $[C_5R_5]^-$; this was initially recognized by Hawthorne in the syntheses of the first metallacarboranes [6]. There are two

* Corresponding authors. Fax: +1 815 753 4802 (N.S. Hosmane).
E-mail addresses: hosmane@niu.edu (N.S. Hosmane), zhu_yinghuai@ices.a-star.edu.sg (Z. Yinghuai), jmaguire@mail.smu.edu (J.A. Maguire), kaim@iac.uni-stuttgart.de (W. Kaim), takagaki@bnct.jp (M. Takagaki).

different arrangements of the atoms on the C_2B_3 face, one in which the carbons are next to one another (carbons adjacent) and another in which they are separated by a boron atom (carbons apart). They both seem to bond equally well with metals, but the latter is thermodynamically more stable [4,5]. Analogous to that found for the metallocenes, metallacarboranes have been reported in which the metal group bonds to a single carborane cage, to give half-sandwich compounds, or that occupy vertices of two carboranes, to give full-sandwich (*commo*-) compounds. We have been exploring these compounds as potential catalysts, or catalyst precursors, as well as exploring their use as boron delivery agents in BNCT.
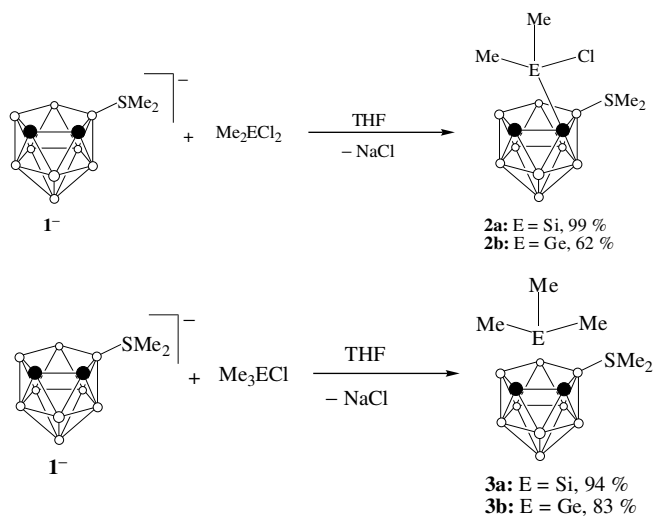
One of the most startling developments in the last few decades, is in the syntheses and catalytic applications of nano-scaled particles prepared from groups 8–10 elements [7]. We have studied the use of these nanoparticle catalysts, derived from the corresponding metallacarborane precursors.

Our results led us to conclude that there remains a wealth of unexplored research that still to be done on the application of metallacarboranes to problems in catalysis and medicine. The most significant results of this research are presented in this account.

2. Chemistry of main group metallacarboranes

Main group metallacarboranes in which a silicon or germanium occupies an apical position above a $[nido\text{-}(RC)_2B_nH_n]^{2-}$ cage are among the earliest reported [5a,b]. These compounds can exist as either half-sandwich or distorted full-sandwich species with the group 14 element, in both +2 and +4 oxidation states, respectively. In the corresponding metallocenes, only the +2 is found. The dinegative charge on the carborane ligands might play a key role in determining the oxidation state of the metal or it may be that the heteronuclear nature of the bonding face is important. Therefore, it is an open question as to what oxidation state would be favored when the group 14 element would bond to a monoanionic carborane ligand, such as a charge-compensated carborane. This curiosity led us to react the charge-compensated ligand, $[9\text{-}SMe_2\text{-}7,8\text{-}C_2B_9H_{10}]^{1-}$ (1^-) with Me_2ECl_2 and Me_3ECl (E = Si, Ge) [8]. Scheme 1 shows that a 1:1 stoichiometric reaction takes place to form $\eta^1\text{-}8\text{-}EMe_2Cl\text{-}9\text{-}SMe_2\text{-}7,8\text{-}C_2B_9H_{10}$ (E = Si(**2a**), Ge(**2b**)) and $(EMe_3)\text{-}9\text{-}SMe_2\text{-}7,8\text{-}C_2B_9H_{10}$, (E = Si(**3a**), Ge(**3b**)) even in the presence of excess carborane [8].

Compounds **2a** and **2b** were found to be isostructural (Figs. 1 and 2) with the $EClMe_2$ group bonded to the cage carbon that is
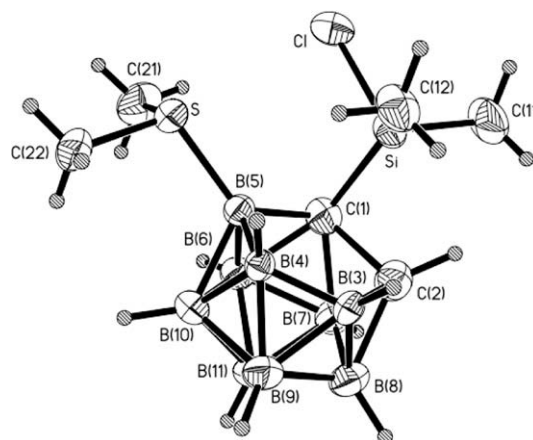

Fig. 1. Crystal structures of group 14 (Si) metallacarboranes.
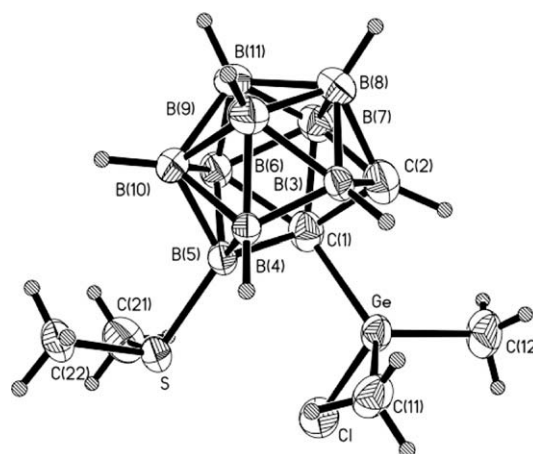

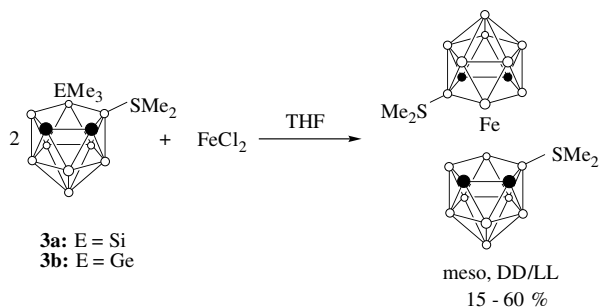**Fig. 2.** Crystal structures of group 14 (Ge) metallacarboranes.

adjacent to the Me_2S–B vertex [8]. A comparison of the structures of **2a** and **2b** with the precursor $[9\text{-}SMe_2\text{-}7,8\text{-}C_2B_9H_{10}]^-$ showed that coordination by the $EClMe_2$ causes a lengthening of the cage carbon bonds from 1.535 Å to 1.818 Å and 1.844 Å, respectively; the C(7)–B(9) bonds are also elongated, from 1.598 Å to 1.792 Å and 1.794 Å (see Fig. 1).

The bonding of the $EClMe_2$ groups to the cage carbon is interesting and atypical in that the carbon atom already has a terminal hydrogen. It is an open question as to whether the 0.3 Å elongation of the C_{cage}–C_{cage} bond constitutes a bond rupture.

It was found that the complex, $(SiMe_3)(9\text{-}SMe_2\text{-}7,8\text{-}C_2B_9H_{10})$, was highly reactive towards other metal halides and is potentially useful as a carborane transfer agent as evidenced by the formation of the corresponding charge-compensated Fe(II)-sandwich complex (Scheme 2). It is of interest that the Fe(II) is sandwiched between two η^5-bonding carboranes, as seen in Fig. 3 [8].

3. Nanoparticles-catalyzed isotopic exchange reactions

Nanoscale metal particles have been attracting much attention and are widely explored for their intriguing chemical and physical properties, as well as potential applications [9]. The extremely high surface areas and the subsequent high density of active sites of these nanoparticles make them more attractive catalysts than the bulk metals [10,11]. Transition metals such as Ru, Os, Ir, and Rh, were found to activate B–H bonds in boron clusters to form metal–boron (M–B) bonds [12]. Also, carboranes and boron hydrides

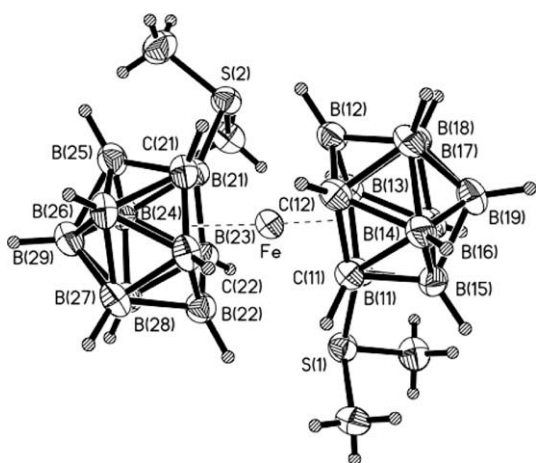**Scheme 1.** Syntheses of group 14 metallacarboranes.

Scheme 2. Reactivity of group 14 metallacarboranes.

were found to undergo catalytic isotopic exchange of their terminal hydrogens with deuterium gas in the presence of $(PPh_3)_3RuHCl$ as catalyst [13]. In view of these examples of B–H activation and the enhanced catalytic activity of nanoscale metal particles, we investigated the possibility of synthesizing ^{10}B enriched decaborane(14) via isotope exchange between natural abundant decaborane(14) and ^{10}B enriched diborane, in the presence of Ru(0) nanoparticles as catalysts [14]. The precursor of the metal catalyst was the bimetallic metallocene complex, $[CpRuCp^*RuCp^*]PF_6$ ($Cp^* = C_5Me_5$) [15], that produced the ruthenium nanoparticles by reduction with hydrogen in a mixed solvent of ethylene glycol and the ionic liquids trihexyltetradecylphosphonium dodecylbenzenesulfonate, [THTdP][DBS], or 1-*n*-Butyl-3-methylimidazolium hexfluorophate, [BMIM][PF₆], as stabilizing agents [14]. The reaction is a two-phase one. Due to the difference in densities of the two ionic liquids, the ionic liquid containing nano-Ru(0) could be either the top layer or the bottom layer of the biphasic mixture. As can be seen from Fig. 4a, the [THTdP][DBS]-stabilized nano-Ru was the upper layer, while in [BMIM][PF₆] it was the lower layer [14]. Since the fluoride containing ionic liquid, [BMIM][PF₆], might release HF under certain reaction conditions, which could cause severe corrosion problems, only the environmental benign ionic liquid, [THTdP][DBS], was used in catalytic runs. Fig. 4b shows that well-dispersed ruthenium nanoparticles with a uniform size (2–4 nm) were obtained from [THTdP][DBS]; these were further analyzed by XRD and XPS, as shown in Fig. 4c–d [14]. The XRD spectra (Fig. 4c) show a bulk Ru(0) model with broad peaks owing to small size. XPS spectra show typical Ru(0) absorptions at 280.08 and 284.48 eV for $3d_{5/2}$ and $3d_{3/2}$, respectively, with an $\Delta = 4.40$ eV; these values were found to be consistent with those reported in the literature [16]. The [THTdP][DBS] protected ruthenium nanoparticles were found to be stable for more than one month under an argon atmosphere.

Fig. 3. Crystal structure of charge-compensated Fe(II)-sandwich complex.

(a) Ru nanoparticles in different ionic liquids

(b) TEM picture of Ru nanoparticles

(c) XRD spectra
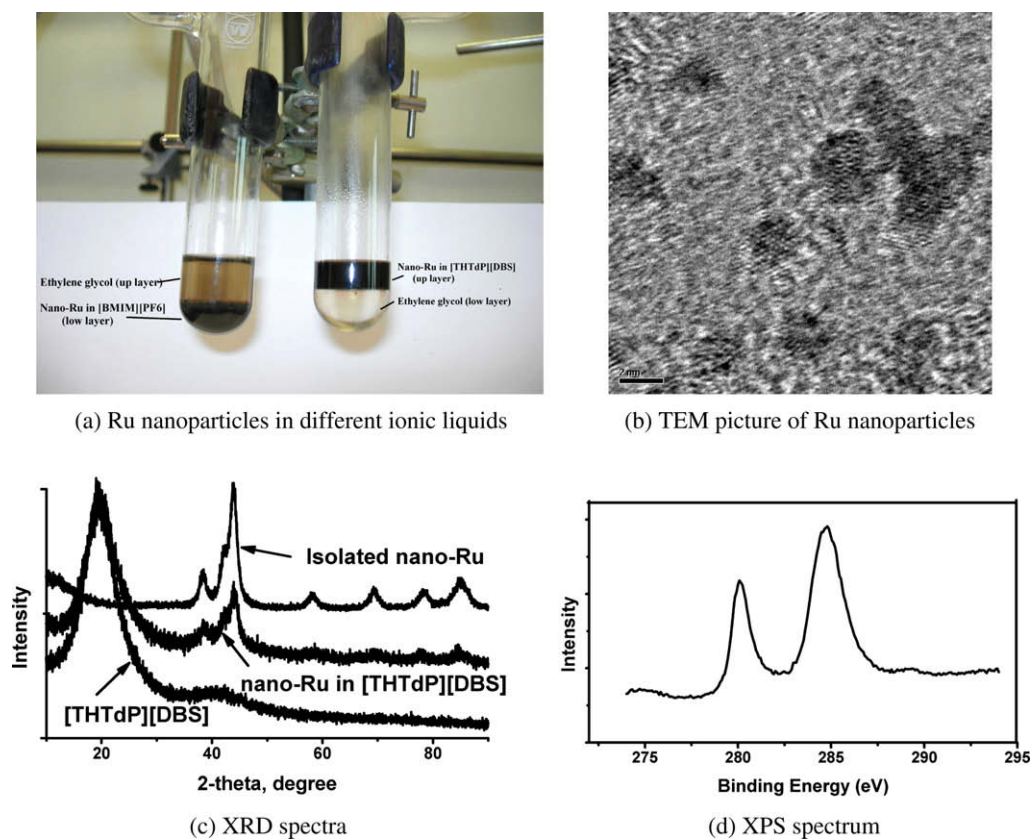

(d) XPS spectrum

Fig. 4. Ionic liquid systems, TEM, XRD and XPS of Ru nanoparticles.

A boron-10 enriched cluster $B_{10}H_{14}$ could be prepared from the boron exchange reaction of ^{10}B enriched diborane ($^{10}B_2H_6$) [17] and natural abundant $B_{10}H_{14}$, catalyzed by the ruthenium nanoparticles dispersed in the ionic liquid, [THTdP][DBS], as outlined in Scheme 3 [14].

The $^{10}B_2H_6$ was introduced to the system and the reaction was continued for 6 h at 50 °C and ca. 1 atm. The procedure was repeated six times for each sample and the products were analyzed by Raman spectroscopy. After purification, it was found that 97.3% of the decaborane(14) was recovered in each enrichment run. The final batch of ^{10}B enriched $B_{10}H_{14}$ was also analyzed with $^{10}B\{^1H$-decoupled$\}$-NMR and MS. The recyclable biphasic catalytic system could be used at least three times without showing obvious changes in activity [14]. The ^{10}B NMR of the final product shows the same peaks as did the ^{11}B NMR of the starting borane, which confirms identical structures for the beginning and final borane clusters. The mechanism of this exchange reaction is not as yet known. However, a likely sequence could involve the decaborane setting down on a Ru(0) with B–H bond cleavage, giving a partially anionic boron species that could then react with a catalyst-bound $^{10}BH_2$ or $^{10}BH_3$ forming a metal bound $nido$-$B_{11}H_{14}^-$ species, in which the ^{10}B could migrate from a facial position to one within the complex. Removable of an unlabelled B vertex would lead to a mono substituted B_{10} cage. This process could be repeated. It should be pointed out that the overall exchange reaction is essentially thermoneutral and the reaction is driven by mass-action.
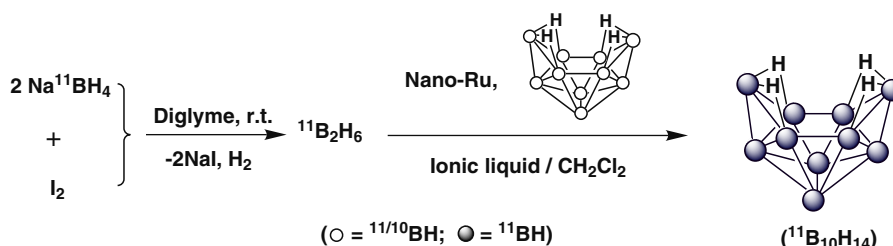
4. Metallacarboranes of constrained-geometry and their catalyric activities

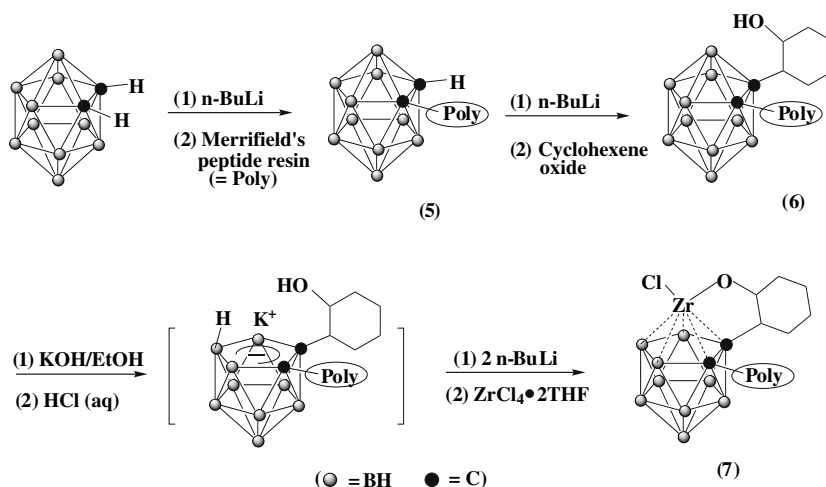In a continuing investigation of the catalytic behavior of constrained-geometry metallacatboranes, we have synthesized K[$nido$-7-Me-8-(2′-hydroxycyclohexyl)-7,8-$C_2B_9H_{10}$, which was then reacted with BuLi in a 1:2 carborane:base molar ratio, to give an intermediate, identified as the trianionic carborane, that reacted with either $ZrCl_4 \cdot 2THF$ or $TiCl_4 \cdot 2THF$ to give the constrained geometry metallacarboranes, $closo$-1-M(Cl)-2-Me-3-(2′-σ-O-cyclohexyl)-η^5-2,3-$C_2B_9H_9$ (M = Zr (**3**), Ti (**4**)). The polymer supported $closo$-1-Zr(Cl)-2-polystyryl-3-(2′-σ-O-cyclohexyl)-η^5-2,3-$C_2B_9H_9$ (**7**) was also synthesized. The polymer substrate was first introduced onto the $closo$-1,2-$C_2B_{10}H_{10}$ by reaction of its lithium salt with Merrifield's peptide resin (1%) to produce 1-polystyrenyl-1,2-$C_2B_{10}H_{11}$, in 88% yield [18]. This compound was reacted $in\ situ$ with n-BuLi and cyclohexene oxide in THF to give the polymer-supported ligand, $closo$-1-polymeryl-2-(2′-hydroxycyclohexyl)-1,2-$C_2B_{10}H_{10}$ (**6**) in 94% yield with the loading amounts up to 1.24 mmol/g (Merrifield's peptide resin (1%)) based on lithium chloride produced (Scheme 4). After decapitation of **6** with potassium hydroxide in refluxing ethanol, followed by deprotonation with n-BuLi in THF, the trianionic intermediate was formed that reacts further with $ZrCl_4\cdot 2THF$ to form the corresponding zirconium complex, $closo$-1-Zr(Cl)-2-polymeryl-3-(2′-σ-O-cyclohexyl)-η^5-2,3-$C_2B_9H_9$ (**7**) with loading amounts of zirconium moiety up to 0.48 mmol/g (Merrifield's peptide resin (1%)) [18].

The polymerization reactions of ethylene and vinyl chloride in the presence of $closo$-1-Ti(Cl)-2-Me-3-(2′-σ-O-cyclohexyl)-η^5-2,3-$C_2B_9H_9$ (**3**) or (**7**) and MMAO-7 cocatalyst were studied. All catalytic runs were carried out in toluene with an [Al]/[Zr] = 2000 at 50 °C under pressures of 1.5 bar of ethylene or 1.2 bar of vinyl chloride. The polymerization data are presented in Table 1 [18].

As can be seen from the table, both **3** and **7**, in the presence MMAO-7 are moderately active catalysts for olefin polymerization, both affording polymers with narrow molecular mass distributions

$$2\ Na^{11}BH_4 + I_2 \xrightarrow[\text{-2NaI, }H_2]{\text{Diglyme, r.t.}} {}^{11}B_2H_6 \xrightarrow[\text{Ionic liquid / }CH_2Cl_2]{\text{Nano-Ru,}}$$

$(\circ = {}^{11/10}BH; \ \bullet = {}^{11}BH)$

$({}^{11}B_{10}H_{14})$

Scheme 3. Catalytic ^{10}B-^{11}B isotope exchange reaction.

(1) n-BuLi / (2) Merrifield's peptide resin (= Poly)

(1) n-BuLi / (2) Cyclohexene oxide

(**5**)　　(**6**)

(1) KOH/EtOH / (2) HCl (aq)

(1) 2 n-BuLi / (2) ZrCl₄•2THF

(**7**)

$(\circ = BH \quad \bullet = C)$

Scheme 4. Synthesis of Merrifield's peptide resin-supported zirconacarborane.

Table 1
Ethylene and vinyl chloride polymerization with **3** (M = Ti) and **7** (M = Zr).

Polymer[a]	Activity[b]	M_w ($\times 10^3$/mol)[c]	M_w/M_n
Polyethylene	53(A) 31(B)	9.4(A) 3.8(B)	1.8(A) 1.3(B)
Polyvinyl chloride	22(A) 14(B)	2.1(A) 1.3(B)	1.6(A) 1.2(B)

[a] The results (A) are for **3** and (B) for **7**. Polymerization conditions: ratio of catalyst and co-catalyst ([Al]/[Zr]) = 2000; solvent = toluene; temperature = 50 °C; pressure = 1.5 bar (polyethylene) and 1.2 bar (polyvinyl chloride); polymerization time = 4 h.

[b] Activity = kg polymer per mol catalyst per h per bar.

[c] Molecular weight and molecular weight distribution were determined by means of gel-permeation chromatography (GPC: Waters 150 °C) at 145 °C using 1,2,4-trichlorobene as a solvent. The weight average molecular weight and polydispersity index (M_w and M_w/M_n, respectively) were calculated on the basis of polystyrene standards.

Fig. 6. Molecular geometries of the iridacarborane precursor for Ir(0) nanoparticles and the corresponding ionic liquid used.

(M_w/M_n = 1.2–1.8) [18]. Even though the activity of the homogeneous olefin (ethylene) is greater than that of vinyl chloride, the activity of the latter is sufficiently high to warrant further investigations of these systems, including their mechanisms.

5. Catalytic arylborylation

We have developed an interest in the catalytic arylborolation reactions using iridium based catalysts. As part of this investigation, several iridium(I) salicylaldiminato–cyclooctadiene complexes of the form, Ir(sal = N-R)(cod) (sal = salicyladehyde; R = CH$_2$Ph (**1**), Ph (**2**); cod = 1,5-cyclooctadiene) (see Figs. 5 and 6 for their crystal structures), have been synthesized, thoroughly characterized, and used as catalysts for arylborylation *via* C–H activation [19]. The highest isolated yield of 91%) was obtained in the presence *tetra*-2-pyridinylpyrazine under reflux condition using catalyst **1**, as outlined in Scheme 5. Our results are comparable with those reported in the literature [20]. The catalytic system could be recycled several time without any noticeable loss of activity.

In a parallel study, well dispersed iridium(0) nanoparticles, stabilized with the ionic liquid, trihexyltetradecylphosphonium methylsulfonate, [THTdP][MS], were prepared by the reduction of the precursor hydridoiridium carborane, (Ph$_3$P)$_2$Ir(H)(7,8-*nido*-C$_2$B$_9$H$_{11}$) (see Fig. 6) [21]. The iridium nanoparticles were found to be active catalysts for arylborylation [19–21] forming boronic acid derivatives (Scheme 6). The activity of the catalyst has been investigated as a function of the activating base, and reaction conditions. The highest yield of 91% was achieved in a microwave
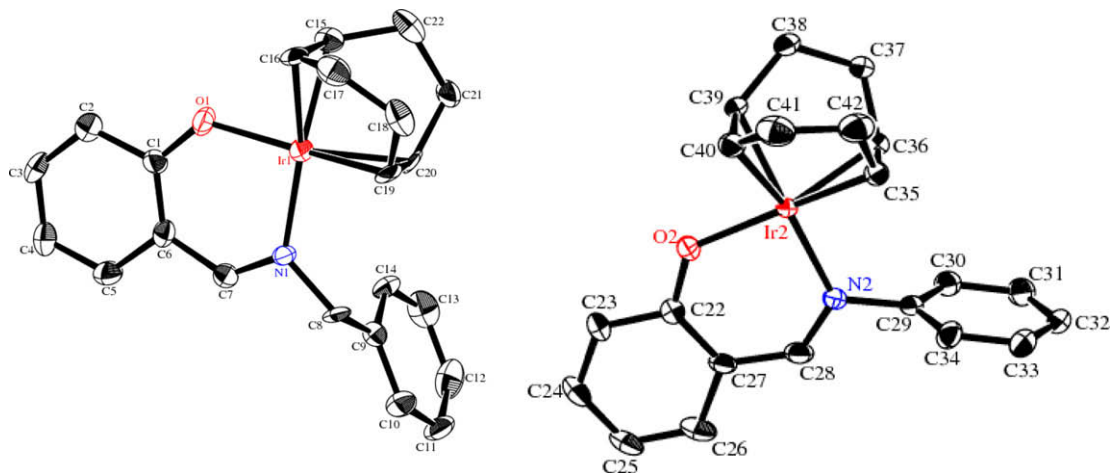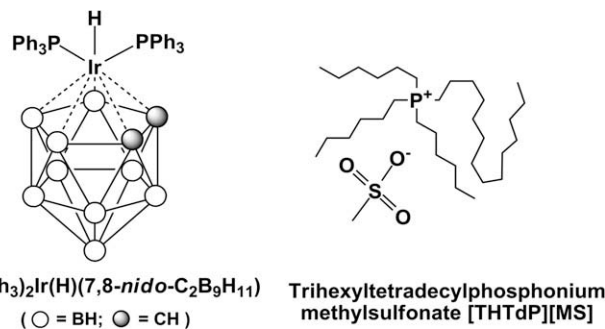
reactor using the base, *tetra*-2-pyridinylpyrazine, in the presence of [THTdP][MS]. Since both the iridium(0) and the iridium(I)-salicylaldiminato–cyclooctadiene catalysts were activated by *tetra*-2-pyridinylpyrazine, it is possible that the true catalyst was some residual (Ph$_3$P)$_2$Ir(H)(7,8-*nido*-C$_2$B$_9$H$_{11}$).

To test this possibility, parallel catalytic studies were carried out on both the (Ph$_3$P)$_2$Ir(H)(7,8-*nido*-C$_2$B$_9$H$_{11}$) precursor and the Ir(0) nanoparticles. The results showed that the precursor exhibited catalytic activity only after an incubation period of ∼4 h, while the Ir(0) nanoparticles were immediately active [21]. At present, we are investigating the nature of the catalytic species produced during the incubation period.

6. Carborane-appended star-shaped clusters

Symmetrical star shaped molecules with carborane clusters on the periphery have been synthesized in good yields *via* silicon tetrachloride mediated cyclotrimerization reactions of the 9-benzyl derivatives of carboranes with an acetyl group substitution on the benzene ring (see Scheme 7 and Fig. 7) [22]. Functionalization of these symmetrical core structures with either 1-iodoheptane and trivinylchlorosilane produced compounds which could be used as precursors for synthesis of higher order carbosilane dendrons, as well as liquid crystalline substances.

This work demonstrates that that an acetyl aromatic moiety attached to the boron atom of the carborane cages will undergo trimerization reactions to generate symmetric building blocks for synthesis of higher order dendrimers or liquid crystalline substances, as well as metallacarboranes and new BNCT agents.

Fig. 5. Molecular structures of **1** (left) and **2** (right).
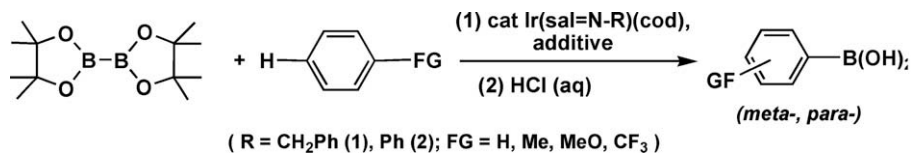
Scheme 5. Iridium(I) salicylaldiminato–cyclooctadiene complexes catalyzed borylation.
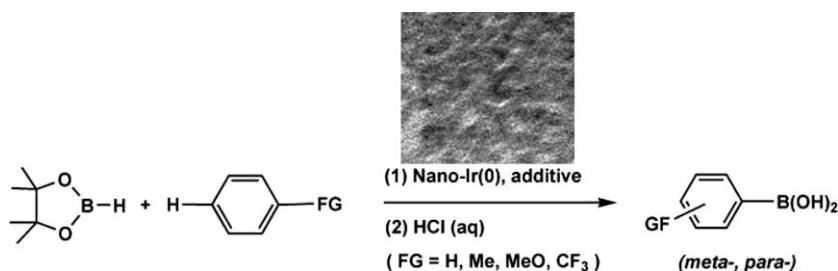
Scheme 6. Iridium(0) nanoparticles-catalyzed phenylborylation.
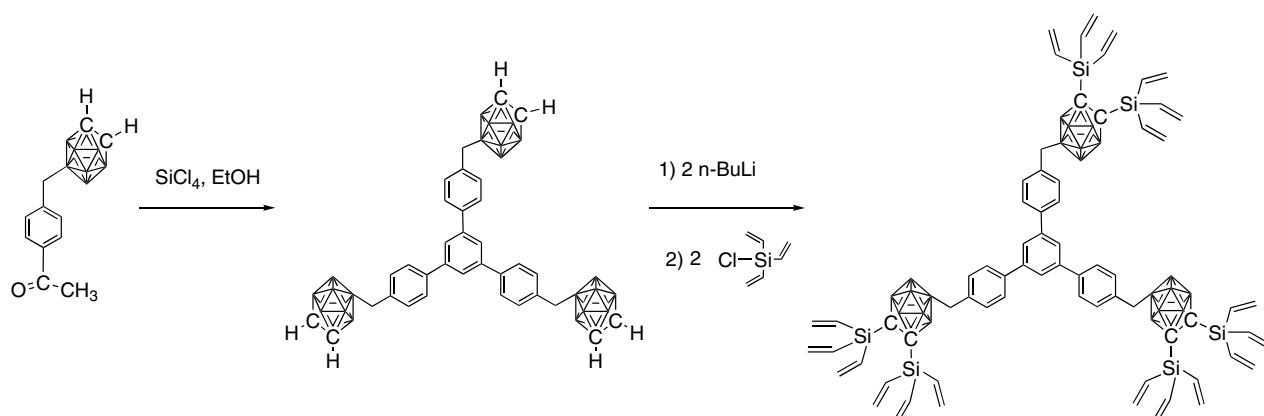
Scheme 7. Synthesis and reactivity of 1,3,5-*Tris*(1,2-dicarba-*closo*-docecacarboran-9-yl)benzene (**4**).
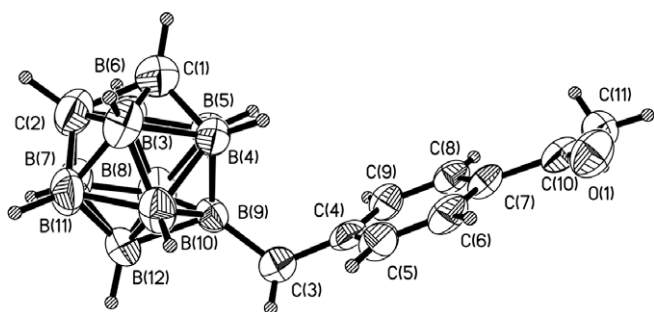

Fig. 7. Crystal structure of the precursor 9-benzyl derivative of ortho-carborane.

Dendrimers can either be prepared using a divergent or a convergent approach. In the divergent method dendrimers are made in a step wise manner from a small polyfunctional core, whereas in the convergent approach the growth of the molecule starts from the periphery and finally attached to the core moiety [23]. The present study has opened a way to synthesize dendritic structures by both convergent and divergent approaches. Scheme 7 illustrates that a new class of carborane containing carbosilane dendrons can also be synthesized starting from **4** and lithiated carboranes *via* hydrosilylation reactions [24]. Furthermore, compounds **4** can be used to make a new class of metallacarboranes via decapitation

of carborane cages [25]. A new generation of BNCT agents may be possible by making these compounds water soluble [26]. Further work is presently underway in our laboratories.

7. Nanotechnology in cancer therapy

Boron neutron capture therapy (BNCT) is a binary cancer treatment in which compounds containing ^{10}B are selectively introduced into tumor cells and then irradiated with thermal neutrons. The ^{10}B nucleus then absorbs a neutron forming an excited ^{11}B nucleus that undergoes a rapid fission reaction, producing a high energy α-particle (1.47 MeV) and ^{7}Li ion (0.84 MeV), in addition to a low energy gamma γ-ray (478 keV). The linear energy transfer (LET) of these heavily charged particles have a range of about one cell diameter [27], which confines radiation damage to the cell from which they arise, hence minimizing cytotoxic effects on the surrounding tissue. The attractiveness of BNCT, and the burden placed on boron delivery agents, lies in the fact that boron heavily localized in a tumor cell can selectively kill the cancer but have minimal effect on the boron free tissues. It has been estimated that a safe, effective dose of a BNCT agent would deliver 20–30 µg ^{10}B/g tumor or $\sim 10^{9}$ ^{10}B atoms per cancer cell, with neighboring healthy cell having considerably less of the boron species (<5 µg ^{10}B/g of cell). Thus, for a boron delivery agent to be effective it must be selectively taken up by the cancer cell. There has been
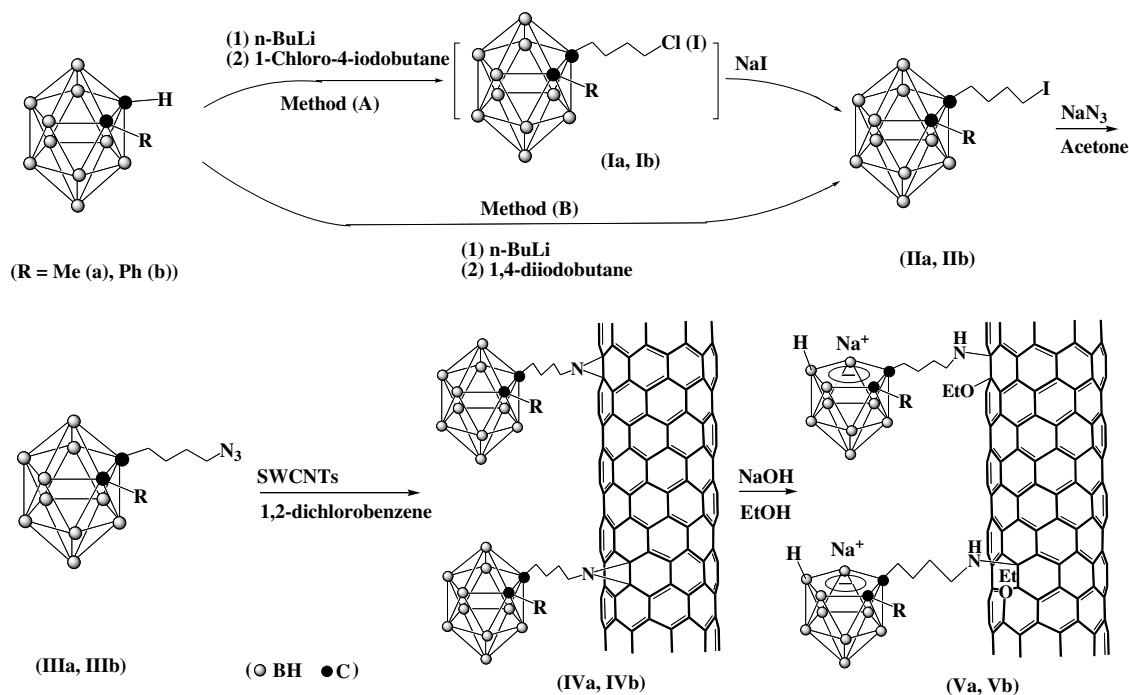
Scheme 8. Synthesis of carborane attached SWCNT [30].

and continue to be a great deal of work needs to be done in developing such agents [27,28].

We took advantage of the fact that functionalized single wall carbon nanotubes (SWCNT's) were able to cross cell membranes and concentrate in a number of neoplastic cells without obvious toxic effects [29]. Thus, the *nido*-carboranes were attached to the side walls of SWCNT's to produce water soluble macromolecular boron carriers, as shown in Scheme 8 [30]. When compound **Va** in Scheme 8 was injected into mice bearing a EMT6 mammary cancer tumor, it was found that the boron persisted in the tumor cell giving a 21.5 B/g tumor and a tumor-to-blood ratio of 3.12:1 [30].

The use of coupling boron rich entities to macromolecules with different properties offers various unique approaches to BNCT therapy for cancer. One example is magnetically directed drug delivery. One of the continuing problems in any drug delivery system is localizing the concentration of the therapeutic agent in the vicinity of the tumor, while avoiding healthy tissue. One way of accomplishing this is to attach the drug to a biocompatible magnetic nanoparticle and use an external magnetic field to direct the particle. It was shown that iron oxide magnetic particles (ferrofluids (FF)) stabilized by a starch polymer, and bound to the anticancer drug mitoxantrone (mtx) proved extremely effective in the treatment of squamous cell carcinoma implanted in the flank of rabbits, when guided by an external magnetic field [31]. These investigators found that this approach led to complete tumor remission with reduced doses of 20–50% FF-mtx. On the other hand the same doses of mtx without magnetic guidance resulted in no decrease in tumor volume [31]. Such magnetically directed approach is currently underway in our laboratories [32].

Another macromolecular approach to delivering large amounts of boron to a tumor is to use boron nano structures (nanotubes, nanoribbons or nanowires) as the primary boron delivery vehicle. These materials are just in their formative stage and problems such as water solubility and toxicity must be addressed. It is of interest to note that the low temperature synthesis of surface functionalized boron nanoparticles have recently been reported [33]. Such structures could be developed into tumor targeting agents for BNCT.

References

[1] (a) K. Wade, Adv. Inorg. Chem. Radiochem. 18 (1976) 1–66;
(b) M. E. O'Neill, K. Wade, Comprehensive organometallic chemistry, in: G. Wilkinson, F.G.A. Stone, E. W. Abel, N.Y. Pergamon (Eds.), vol. 1, 1982, pp. 1–41 (Chapter 1);
(c) R.E. Williams, Adv. Inorg. Chem. Radiochem. 18 (1976) 67–142;
(d) R.E. Williams, Chem. Rev. 92 (1992) 177–207.
[2] D.M.P. Mingos, Acc. Chem. Res. 17 (1984) 311–319.
[3] (a) D.M.P. Mingos, D.J. Wales, Introduction to Cluster Chemistry, Prentice-Hall, Englewood Cliffs, NJ, 1990 (Chapter 2);
(b) E.D. Jemmis, M.M. Balakrisnaranjan, P.D. Pancharatna, J. Am. Chem. Soc. 123 (2001) 4313–4323;
(c) E.D. Jemmis, M.M. Balakrisnaranjan, P.D. Pancharatna, Chem. Rev. 102 (2002) 93–144;
(d) J.E. Demmis, E.G. Jayasree, Acc. Chem. Res. 36 (2003) 816–824.
[4] (a) For general references see: various authors in G. Wilkinson, F.G.A. Stone, E.W. Abel (Eds.), Comprehensive Organometallic Chemistry(I), vol. 1, Pergamon, NY, 1982;
(b) E.W. Abel, F.G.A. Stone, G. Wilkinson (Eds.), COMC II, vol. 1, Elsevier Science, Oxford, UK, 1995;
(c) R.H. Crabtree, D.M.P. Mingos (Eds.), COMC-III, vol. 3, Elsevier, Oxford, 2006;
(d) G.A. Olah, K. Wade, R.E. Williams (Eds.), Electron-Deficient Boron and Carbon Clusters, Wiley, New York, 1991;
(e) M. Davidson, A.K. Hughes, T.B. Marder, K. Wade (Eds.), Contemporary Boron Chemistry, Royal Society of Chemistry, London, 2000;
(f) in: J. Casanova, (Ed.) Borane, Carborane, Carbocation Continuum, Wiley, New York, 1998.
[5] (a) J. Wang, J.A. Maguire, N.S. Hosmane, in: ACS Symposium Series, vol. 917 (Modern Aspects of Main Group Chemistry), 2006, pp. 293–309;
(b) N.S. Hosmane, J.A. Maguire, Organomeatllics 24 (2005) 1356–1389;
(c) L. Deng, Z. Xie, Z. Organomet. 26 (2007) 1832–1845;
(d) Metallacarboranes with other values of *n* are known [4], but this report will concentrate mainly on those in which *n* = 4 and 9 N.M.M. Wilson, D. Ellis, A.S.F. Boyd, B.T. Gilles, S.A. Macgregor, G.M. Rosiar, A.J. Welch, Chem. Commun. (2002) 464–465.

[6] M.F. Hawthorne, D.C. Young, P.A. Wegner, J. Am. Chem. Soc. 87 (1965) 1818–1819.
[7] Z. Yinghuai, L.C. Nong, H. Yifan, N.S. Hosmane, J.A. Maguire, Chem.: An Asian J. 3 (2008) 650–662.
[8] V. Meshcheryakov, C. Zheng, A.R. Kudinov, J.A. Maguire, N.S. Hosmane, Organometallics 27 (2008) 5033–5037.
[9] (a) D. Schmid, Clusters and Colloids, VCH Press, New York, 1994;
(b) A. Furstner, Active Metals, VCH, Weinheim and New York, 1996.
[10] (a) R.G. Finke, Transition-metal nanoclusters: solution-phase synthesis, then characterization and mechanism of formation, of polyoxoanion- and tetrabutylammonium-stabilized nanoclusters, in: D.L. Feldheim, C.A. Foss Jr. (Eds.), Metal Nanoparticles: Synthesis, Characterization and Application, Marcel Dekker, New York, 2002, pp. 17–54;
(b) L.N. Lewis, Chem. Rev. 93 (1993) 2693–2730.
[11] (a) R. Narayanan, M.A. El-Sayed, J. Phys. Chem. B 109 (2005) 12663–12676;
(b) B.F.G. Johnson, Coord. Chem. Rev. 190–192 (1999) 1269–1285;
(c) B.V. Ershov, Rossiiskii Khimicheskii Zhurnal 45 (2001) 20–30;
(d) A. Roucoux, J. Schulz, H. Patin, Chem. Rev. 102 (2002) 3757–3778;
(e) M. Moreno-Manas, R. Pleixats, Acc. Chem. Res. 36 (2003) 638–643;
(f) N. Pernicone, CATTECH 7 (2003) 196–204;
(g) W. Qiang, A.E. Ostafin, Encyclopedia of nanoscience and nanotechnology 5 (2004) 475–503.
[12] (a) M. Herberhold, H. Yan, W. Milius, B. Wrackmeyer, Chem.-A Eur. J. 8 (2002) 388–395;
(b) B. Wrackmeyer, H. Yan, W. Milius, M. Herberhold, Russ. Chem. Bull. 50 (2001) 1518–1524;
(c) M. Herberhold, H. Yan, W. Milius, B. Wrackmeyer, Chem.-A Eur. J. 6 (2000) 3026–3032;
(d) A.F. Hill, G.R. Owen, A.J.P. White, D.J. Williams, Angew. Chem., Int. Ed. Engl. 38 (1999) 2759–2761.
[13] E.L. Hoel, M. Talebinasab-Savari, M.F. Hawthorne, J. Am. Chem. Soc. 99 (1977) 4356–4367.
[14] Y. Zhu, E. Widjaja, S.L. Pei-Sia, W. Zhan, K. Carpenter, J.A. Maguire, N.S. Hosmane, M.F. Hawthorne, J. Am. Chem. Soc. 129 (2007) (2007) 6507–6512.
[15] A.R. Kudinov, M.L. Rybinskaya, Y.T. Struchkov, A.I. Yanovskii, P.V. Petrovskii, J. Organomet. Chem. 336 (1987) 187–197.
[16] J.F. Moulder, W.F. Stickle, P.E. Sobol, K.D. Bomben, Hand book of X-ray Photoelectron Spectroscopy, Physical Electronics Inc., USA, 1995. 114-115.
[17] C. Narayana, M. Periasamy, J. Organomet. Chem. 323 (1987) 145–147.
[18] Y. Zhu, Z. Yulin, K. Carpenter, J.A. Maguire, N.S. Hosmane, J. Organomet. Chem. 690 (2005) 2802–2808.
[19] Y. Zhu, K.C. Yan, L. Jizhong, C.S. Hwei, Y.C. Hon, A. Emi, S. Zhenshun, M. Winata, N.S. Hosmane, J.A. Maguire, J. Organomet. Chem. 692 (2007) 4244.
[20] R.E. Maleczka Jr., F. Shi, D. Holmes, M.R. Smith III, J. Am. Chem. Soc. 125 (2003) 7792.
[21] Y. Zhu, K. Chenyan, A.T. Peng, A. Emi, W. Monalisa, N.S. Hosmane, J.A. Maguire, Inorg. Chem. 47 (2008) 5756.
[22] B.P. Dash, R. Satapathy, J.A. Maguire, N.S. Hosmane, Org. Let. 10 (2008) 2247.
[23] J.-P. Majorial, A.-N. Caminade, Chem. Rev. 99 (1999) 845.
[24] (a) R. Nunez, A. Gonzalez-Campo, A. Anna Laromaine, F. Teixidor, R. Sillanpaa, R. Kivekas, C. Vinas, Org. Lett. 8 (2006) 4549;
(b) R. Nunez, A. Gonzalez, C. Vinas, F. Teixidor, R. Sillanpaa, R. Kivekas, Org. Lett. 7 (2005) 231;
(c) Nunez, A. Gonzalez-Campo, C. Vinas, F. Teixidor, R. Sillanpaa, R. Kivekas, Organometallics 24 (2005) 6351.
[25] (a) J. Thomas, M.F. Hawthrone, Chem. Commun. (2001) 1884;
(b) J. Yoo, J-W. Hwang, J.-W. Do, Inorg. Chem. 40 (2001) 568;
(c) C. Vinas, R. Benakki, P. Angles, H. Meliani, F. Teixidor, R. Kivekas, R. Sillanpaa, J. Organomet. Chem. 570 (1998) 79.
[26] K. Vyakaranam, G. Rana, A. Ratanasuwan, S.N. Hosmane, J.A. Maguire, N.S. Hosmane, Organometallics 21 (2002) 3905.
[27] A.H. Soloway, W. Tjarks, B.A. Bauman, F.-G. Rong, R.F. Barth, I.M. Codogni, J.G. Wilson, Chem. Rev. 98 (1998) 1515 and references therein.
[28] M.F. Hawthorne, M.W. Lee, J. Neuro-oncol. 62 (2003) 33.
[29] (a) D. Pantarotto, J.-P. Briand, M. Prato, A. Bianco, Chem. Commun. (2004) 16;
(b) P. Cherukuri, S.M. Bachilo, S.H. Litovsky, R.B. Weisman, J. Am. Chem. Soc. 126 (2004) 15638;
(c) N.W.S. Kam, T.C. Jessop, P.A. Wender, H. Dai, J. Am. Chem. Soc. 126 (2004) 6850.
[30] Y.H. Zhu, T.P. Ang, K. Carpenter, J.A. Maguire, N.S. Hosmane, M. Takagaki, J. Am. Chem. Soc. 127 (2005) 9875.
[31] C. Alexiou, W. Arbold, R.J. Klien, F.G. Parak, P. Hulin, C. Bergemann, W. Erhart, S. Wagenpfeil, A.S. Lübbe, Cancer Res. 60 (2000) 6641.
[32] (a) Y. Zhu, US Patent Application #60/737, 827 (WO/2007/058630);
(b) Y. Zhu, J.A. Maguire, N.S. Hosmane, submitted for publication.
[33] A.L. Pickering, C. Mitterbauer, N.D. Browing, S.M. Kauzlarich, P.P. Power, Chem. Commun. (2007) 580.